Modular Artificial Neural Networks for Wireless Power Transfer Optimization in Sensor-Driven Industrial IoT

Modular Artificial Neural Networks for Wireless Power Transfer Optimization in Sensor-Driven Industrial IoT

Elisa Augello
DEI "Guglielmo Marconi"
University of Bologna
Bologna, Italy
elisa.augello2@unibo.it

Diego Masotti
DEI "Guglielmo Marconi"
University of Bologna
Bologna, Italy
diego.masotti@unibo.it

Alessandra Costanzo
DEI "Guglielmo Marconi"
University of Bologna
Bologna, Italy
alessandra.costanzo@unibo.it

***Abstract*— This work presents a novel approach, utilizing modular Artificial Neural Networks (ANNs), to model complex and confined electromagnetic (EM) environments, when the far-field approximation is inadequate. The main objective is to optimize energy harvesting and sensor placement within Wireless Power Transfer (WPT) systems, which are crucial for the autonomous functioning of Wireless Sensor Networks (WSNs) in harsh EM environments. To enhance computational efficiency, the Integral Solver method is adopted to create parameterized EM simulation scenarios, for the generation of the training data. Additionally, an active learning algorithm is employed to identify an optimal, minimal dataset for training and testing the modular ANN architecture. This architecture comprises distinct sub-networks aimed at predicting both optimal sensors spatial coordinates and maximum power density levels. The evaluation of these sub-networks demonstrates the effectiveness of ANN-based methods in tackling the challenges associated with WPT optimization for WSN applications in demanding EM environments.**

Keywords—Wireless Power Transfer, Wireless Sensor Networks, Artificial Intelligence

I. Introduction

The Industrial Internet of Things (IIoT) is gaining attention for its ability to enhance connectivity among systems, machines, and sensors in critical environments like automotive, manufacturing, and healthcare [1]. In this context Wireless Sensor Networks (WSNs) enable functionalities, such as remote monitoring and predictive maintenance, but powering the growing number of IIoT sensors via traditional wiring is impractical. Wireless Power Transfer (WPT) and Energy Harvesting (EH) become essential for sensor autonomy allowing continuous operation and improving scalability. However, many industrial environments are electromagnetically (EM) complex, with obstacles and materials causing unpredictable EM field behavior, complicating the channel model definition [2]. Nevertheless, accurate power density estimation is critical for maintaining reliable WPT links and ensuring sufficient energy for battery-free sensors. In [3] it was shown that sensors' charging time exhibits a non-trivial dependence on their position relative to RF illuminators, highlighting the need to consider environmental factors, like operating frequency, obstacles, and material properties, for optimal co-location of sources and sensors [4]. Additionally, predicting the power density at the sensors locations is crucial for estimating energy harvesting capacity and charging time [5]. This emphasizes the need for advanced prediction methods, and, in particular, Artificial Neural Networks (ANNs) emerge as a powerful tool to reveal complex relationships and to address the limitations of traditional modeling methods [6]. In this work the analysis of a technique to characterize a generic parametrized environment using an ANN is presented. In Section II an optimized simulation method for the generation of training data is presented. In section III a smart algorithm to strategically select the most informative data is described, followed by the ANN description and its results, in Section IV and in Section V conclusions are drawn.

II. Simulation Method for the Training Set Generation

Selecting the right EM simulator engine is crucial for WSNs applications in industrial environments. These environments are often electromagnetically large, making traditional full-wave simulators time-consuming and prone to convergence issues and reduced accuracy. While ray-tracing and Friis models are effective in some cases, they may fail when the far-field approximation is invalid. Indeed, in industrial scenarios, components and systems monitored by sensors may also be in the near-field or mid-field relative to the RF source. Therefore, the simulation technique selected must be reliable in every operative region. To overcome this issue the proposed method is based on the Integral Equation (IE) solver [7] and minimizes the simulation time while providing the required level of accuracy. This is obtained exploiting a surface meshing rather than a volumetric one as traditional full-wave frequency domain (FD) simulators. Surface meshing is particularly useful for WSN deployments, where multi-scale problems arise due to varying obstacle

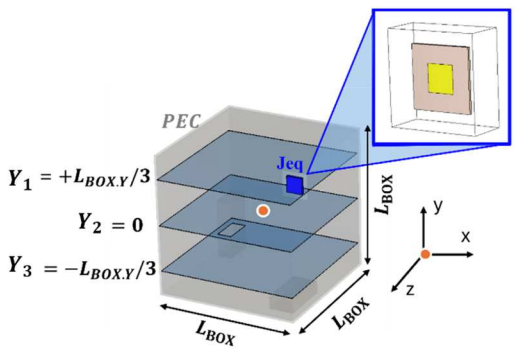

Fig.1. Schematic representaion of an eclosed environment filled with obstacles of different shapes and materials in the presence of an RF source. Three equidistant planes are selected for monitoring the power density distribution.

Doi: 10.1109/WPTCE62521.2025.11062219

types and the small size of RF sources used for WPT systems compared to the surrounding environment. To ensure a reliable accuracy and further optimize the simulation time, an equivalent source representation of the actual RF source is used, to avoid the fine-meshing of the source inside the large enclosed scenario. The RF source is first simulated in a predefined bounded volume and represented in the large environment by its equivalent impressed current. This approach provides a more realistic representation of the source EM near-field, offering a higher level of abstraction. The environment under consideration serves as a reference parametrized scenario and is depicted in Fig.1. It has a cubic shape and its walls are made of Perfect Electric Conductor (PEC) with each edge (L_{BOX}) 50 cm long. For the sake of simplicity in this stage of the analysis the dimension of the enclosure, the source and its position are considered as invariant. Leveraging the capabilities of the IE Solver, to compute the EM fields on surfaces, multiple vacuum sensing planes are positioned at various heights of the metallic enclosure for comprehensive monitoring, as showed in Fig.1. The source frequency has been set to 2.45 GHz which is a common choice for WSNs.

III. DATA SELECTION

The generic EM environment in Fig.1 contains j=1,…,K objects which are parallelepiped-shaped for the sake of simplicity and parametrized through N_D descriptive variables, specifically volumes V_j, volumes'centers $C_j = \{x_j, z_j\}$ and materials m_j. These have been chosen arbitrarily, as detailed in [8], and can be expanded for a better description of the environment, to cover other configurations. An additional parameter considered during the sampling procedure is the relative volumetric occupation (VO) of the obstacles present in the given environment, which is computed as:

$$VO = \frac{\sum_{j=1}^{K} V_j}{V_{BOX} - \sum_{j=1}^{K} V_j} \quad (2)$$

measuring the fraction of space occupied, relative to the overall available volume (the box volume) . The vector $D^T = \{D_1, \dots, D_j, \dots D_K\}$ with $D_j = \{V_j, x_j, z_j, m_j\}$ is descriptive of the overall parametrized environment, containing K obstacles, each one described by N_D variables. Each D^T vector corresponds to an environment which will be EM-simulated to retrieve the corresponding power density distribution. For many practical applications it is often straightforward to automatically collect a vast amount of unlabeled data, commonly referred to as "candidate set". Nevertheless, assigning labels – i.e. assigning the ground truth to given input variables set – can be a highly time-consuming process, as well as resource-intensive, particularly when each label requires the running of an EM simulation. The minimum number of the D^T sets is selected to be representative of a real scenario to reduce the overall computational load. To address this challenge an active learning algorithm is proposed, with the objective of iteratively selecting an "active pool" of representative data to be "labeled" [9]. The generic element of vector D^T, of dimensionality $N_D \cdot K$, is sampled $i = 1, \dots, N$ times by means of Latin Hypercube Sampling (LHS), obtaining a large set of candidates. To ensure consistency with real scenarios the unfeasible combinations giving rise to objects overlap, or volumes exceeding the boundaries, are filtered out. To the resulting candidates set the active sampling algorithm is applied, optimally selecting the most informative samples, to be labeled by means of the following procedure. K-means clustering [10] is applied to group similar samples, representing EM environments, into M clusters. As initialization step, the clusters centers are added to the active pool and then subsequently updated. For each of the M clusters, an optimally selected sample is retrieved and inserted in the active pool, considering its diversity with respect to the already selected samples present in the active pool and its representativeness with respect to its cluster. Let $S_{C_m,i}$, be the generic $N_D \cdot K$ sample belonging to the cluster C_m, two associated figures of merits (FoM) are defined: representativness, G_R, and diversity G_D. Representativeness is defined as:

$$G_R(S_{C_m,i}) = \frac{1}{N_m - 1} \times \sum_{S_{C_m,i} \in C_m} \left\| S_{C_m,i} - S_{C_m,k_{(k \neq i)}} \right\| \quad (2)$$

with i, k=1,…, N_m, and N_m = number of elements in the cluster. This metric compares a sample with the others in the same group and measures how central it is relatively to the cluster. Diversity is defined as:

$$G_D(S_{C_m,i}) = \min_{l,m \in [1,\dots,M], m \neq l} \left\| S_{C_m,i} - S_{C_l}^{OPT} \right\| \quad (3)$$

with i=1,…, N_m considering the minimum distance among a sample in the cluster C_m and the other optimally selected samples in the rest of the clusters, which are already in the active pool. A trade-off between (2) and (3), is then derived:

$$S_{C_m,i}^{OPT} = \arg\max[G_D(S_{C_m,i}) - G_R(S_{C_m,i})] \text{ , i=1,…, } N_m. \quad (4)$$

to ensures that the selected EM environments are distinct enough from one another while still being representative of their respective clusters. For each cluster, this samples selection procedure can be iterated from the initialization step consisting of the previously selected M samples in the active pool. At the end of each generic iteration n the optimally selected samples $M^{(n)}$ are labelled by means of EM simulation and used to train an ANN, allowing the addition of new samples until the desired accuracy level is reached.

IV. MODULAR ARTIFICIAL NEURAL NETWORK

As a reference scenario the square metallic enclosure of side L_{BOX} is filled with two obstacles (K=2) with varying dimensions and materials. Their volumes V_j are distributed over the ranges [8,6000] cm^3, while the volumes centers $C_j = \{x_j, z_j\}$ covers the various positions in the entire environment. Additionally, the materials m_j of these volumes are limited to binary values corresponding to PEC and FR-4 ($\varepsilon_r = 4.3, \tan\delta = 0.025$). From an initial candidates set of 10000

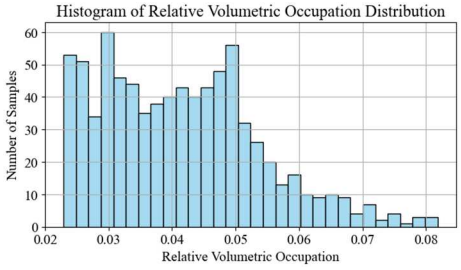

Fig.2. Relative Volumetric Occupation (VO) distribution of selected volumes in the active pools, for the reference scenario of Fig. 1.

samples (generated by linearly varying over the selected intervals the variables described above), active pools are iteratively extracted using (4). n=8 iterations have been carried out, optimally selecting M=100 samples, resulting in a total of N_s=800 samples. The resulting relative volumetric occupation VO is reported in Fig. 2, showing how the algorithm is designed to select a representative range of volumetric occupation values. Combinations of obstacle volumes that result in higher volumetric occupation values are less likely to be chosen due to geometric constraints, such as the occurrence of spatial intersections or overlap between obstacles, which renders those configurations infeasible. The optimally selected samples are labelled by means of CST Microwave Studio with the simulation approach described in Section II, to retrieve the power density distribution in the specified environment and the correspondent optimal sensor location. To model the relationship between input parameters and labeledd data, a modular set of ANNs was employed. The chosen architecture, shown in Fig.3, consists of four parallel neural networks that take as input the description of the EM environment in the form of the descriptive vector D^T, for a total of $K \cdot N_D = 8$ variables. The neural networks ANN_X and ANN_Z predict the coordinates x_{max} and z_{max}, respectively, where the maximum power density level are expected, and represent the ideal sensor position. The value of maximum power density, P_{max}, is predicted by the neural network ANN_P. Finally, the ANN_Y predicts plane y_{max} on which P_{max} is sensed.

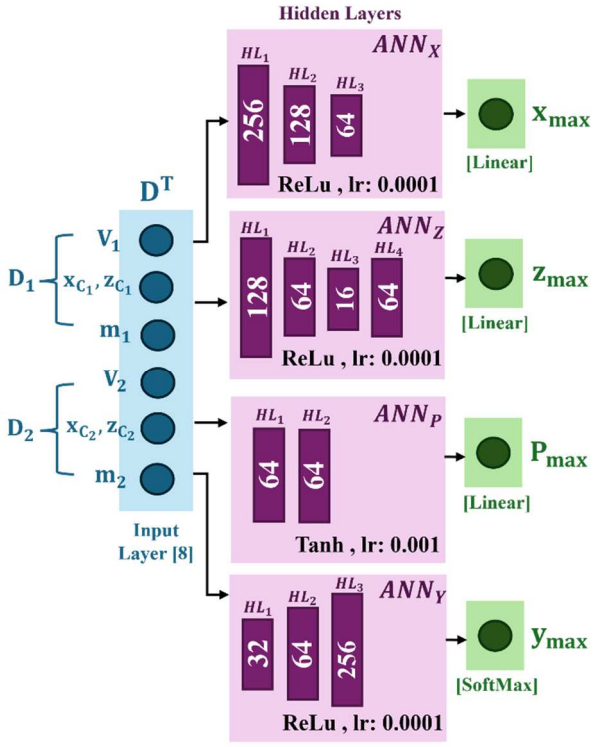

Fig. 3. Schematic representation of the implemented ANN architecture for simultaneous prediction of maximum power density (P_{max}) and its location, in terms of coordinates $\{x_{max}, z_{max}\}$, and reference plane y_{max}.

This modular approach allows each neural network to specialize in learning the most relevant features for its specific task, offering the flexibility to optimize each network individually. As a result, it achieves higher accuracy compared to a single unified ANN architecture. A preprocessing step consisting of Min-Max scaling has been carried out in order to ensure that entire dataset is rescaled into a consistent interval. Thus each generic sample in D^T is normalized as $D_{scaled} = (D - D_{min})/(D_{max} - D_{min})$ considering the respective minimum and maximum values. Similarly, a scaling procedure is applied separately to the network outputs to ensure consistency and compatibility with the training data. This normalization ensures that the predicted values fall within the same range as the normalized targets, improving training stability and accuracy. Subsequenty, an optimization procedure applied separately to the four networks is performed using grid search combined with Optuna [11], a powerful hyperparameter optimization (HPO) framework, exploring different numbers of hidden layers, of neurons per hidden layer, activation functions and learning rate with the final objective of minimizing training and testing losses. The layouts and hyperparameters resulting from the optimization procedure are reported in Fig.3. The ANN_X previews three fully-connected hidden layers respectively with neurons 256, 128 and 64 for the x_{max} prediction. The optimization procedure identified the Rectified Linear Unit (ReLu) [12] activation function as the most suitable, which has a good ability of mitigating vanishing gradient issues, and a learning rate (lr) of 0.0001. The same activation function and learning rate are present in ANN_Z with a layout consisting of four hidden layers respectively with 128,64,16,64 neurons for the z_{max} prediction. The ANN_P network predicting the P_{max} has two hidden layers with 64 neurons each and activation function hyperbolic Tangent [12], trained with a learning rate of 0.001. The learning rates for the sub-networks were optimized based on the specific nature of their tasks and activation functions. For ANN_Z and ANN_x a lower learning rate ensures gradual and stable convergence, which is critical for the precision required in spatial predictions, especially given the sensitivity of these tasks to subtle variations in the input features. Additionally, the ReLU activation function used in these networks benefits from a smaller learning rate to mitigate the risk of instability adjusting its weights and biases by smaller steps during the training process. In contrast, the ANN_P network employs a higher learning rate of 0.001. This choice is justified by the smoother gradients provided by the Tanh activation function, as well as the relatively simpler regression task, which is less sensitive to fine-grained adjustments. These networks are formulated as regression tasks, therefore linear output neurons are used to handle the continuous predicted values. The network predicting the plane on which the maximum power density is sensed, ANN_Y, maintains the ReLU activation function and learning rate 0.0001 with three hidden layers of 32, 64 and 256 neurons. This network is modelled as a classification problem, considering the three sensing planes defined in the reference parametrized environment at Fig.1. The final neuron has a SoftMax activation which converts the output in likelihood probabilities of each class, to effectively model the multi-classification problem. The three classes correspond to the pre-defined sensing planes on which the EM power density is computed reported in Fig.1. All the networks were trained using the Adam Optimizer resulting to have a good handling of large-scale datasets. The accuracy of regression tasks is evaluated using the Root Mean Squared Error (RMSE) which is reported on non-scaled output data for clarity. In this way this metric directly provides a measure of how closely the neural networks predictions align with the actual values for optimal sensor locations and sensed power levels, computing

the average deviation between the predicted and actual value. The RMSE is computed for each output prediction y during the training and validation procedure as:

$$RMSE = \sqrt{\frac{1}{N_S}\sum_{i=1}^{N_S}(y_i^{EM} - y_i^{NN})^2} \quad (5)$$

with N_s number of samples, y_i^{EM} actual value for the i-th sample outcome of the EM simulator and y_i^{NN} is the predicted value from the neural network.

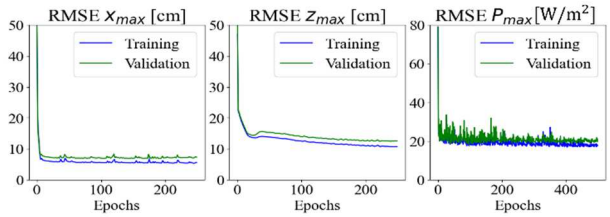

Fig.4. RMSE values for regression tasks x_{max}, z_{max}, P_{max} for training and validation procedure.

The results, presented in Fig.4, are derived by partitioning the initial dataset of 800 samples with an 80%-20% split, where 80% (640 samples) are used for training and 20% (160 samples) are reserved for validation. ANN_X and ANN_Z were trained for 250 epochs, while ANN_P required 500 epochs to reach convergence (an epoch refers to one complete pass through the entire training or validation dataset during which the networks update their weights). The first two networks, which use a learning rate of 0.0001, converged more smoothly, requiring fewer epochs to reach an optimal solution. The third network, with a higher learning rate of 0.001, results in faster but less stable weight updates, requiring more epochs to stabilize and ensure convergence. The higher variability in the output power densities levels further contributes to the need for additional epochs to achieve consistent and reliable performance. These learning rates were empirically validated during the hyperparameter optimization process, demonstrating that tailoring the training dynamics, for each sub-network, leads to improved accuracy and faster convergence across the modular architecture. The final RMSE on validation samples is 6 cm for x_{max} prediction, 10 cm for z_{max} prediction and 20 W/m^2 for P_{max}, with a maximum power density value recorded in the dataset of around 200 W/m^2. The evaluation of ANN_Y on the classification task of y_{max} is carried out by calculating a weighted accuracy (WA) which accounts for the overall class distribution as

$$WA = \frac{\sum_{i=1}^{C}\left(\frac{y_i^{EM}}{y_i^{TOT}} \times y_i^{TOT}\right)}{\sum_{i=1}^{C} y_i^{TOT}} \quad (6)$$

with C=3 number of classes corresponding to the different planes, y_i^{EM} correct classifications for the i-th class and y_i^{TOT} total number of its element. The numerator represents the sum of the weighted percentages of correct classification across all classes, while the denominator is a normalization factor. This metric has been selected to take into account the model's ability to classify but also the classes distribution, that results to be slightly unbalanced. The final WA on the validation set is of 65%, with most of the predictions concentrated in the middle plane, which is closest to the source. Notably, misclassification primarily occurs between adjacent sensing planes in terms of height. To quantitatively assess the prediction accuracy of the trained networks, the location error (LE) and the relative maximum power density error (MPDE) are considered. For each sample i of the validation set, LE is

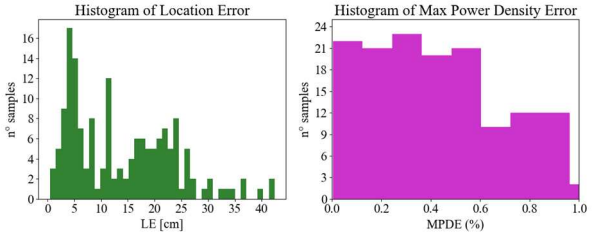

Fig. 5. Histograms of Location Error and Maximum Power Density Error on validation set samples.

computed as the Euclidean distance between the predicted and true coordinates:

$$\text{LE} = \sqrt{(x_i^{NN} - x_i^{EM})^2 + (y_i^{NN} - y_i^{EM})^2 + (z_i^{NN} - z_i^{EM})^2} \quad (7)$$

While the MPDE is computed as:

$$\text{MPDE}\ (\%) = \left|\frac{P_{max_i}^{EM} - P_{max_i}^{NN}}{P_{max_i}^{EM}}\right| \quad (8)$$

considering the absolute difference between the predicted and actual maximum power density value, normalized with

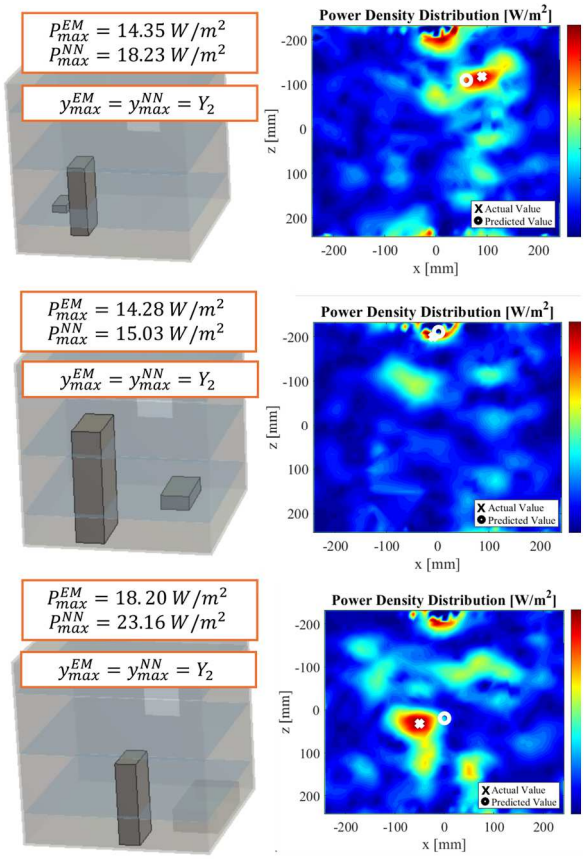

Fig. 6. Predicted power density distributions by the proposed ANN-based EM approach and comparisons between predicted (circles) and actual -full wave simulations- power density maxima locations (crosses) for three different enclosed scenarios

respect to the corresponding labeled data computed by EM simulation. The distribution of the 3D spatial error and of the absolute error on the predicted power density level are reported in Fig. 5. The histograms reveal a peak at low error values indicating that the majority of the predictions are accurate in terms of power and spatially close to the ground truth. Fig. 6 illustrates representative results from the selected validation set, showcasing both the predictions and the corresponding parameterized environments. Three reference scenarios are considered and the actual values outcome of the EM simulations are compared with the predictions of the modular ANN architecture, showing satisfactory results in terms of accuracy.

V. Conclusion

This work demonstrates the potential ANNs as an effective tools for characterizing complex EM environments in WPT applications. A computationally efficient simulation framework was employed, complemented by an active learning algorithm to strategically select informative training samples and reduce the labelling effort of the dataset. By leveraging a modular ANN architecture comprehensive of multiple optimized sub-networks, the proposed method successfully predicts key parameters that determine the optimal sensor location, as maximum power density spatial coordinates and correspondent sensing plane, as well as the sensed power levels. The results highlight the feasibility of using ANN-based methods to address the unique challenges of energy harvesting and sensor placement optimization in WPT-enabled IIoT environments, where EM complexities are prevalent due to obstacles and material diversity. Future work will focus on extending the model's capabilities to dynamically adapt to varying environmental configurations to reach a more scalable solution with respect to the descriptive variables as well as a more complete information in output.

Acknowledgment

This study was carried out within MOST – Sustainable Mobility Center and received fundings from the European Union Next-Generation EU (PNRR – mission 4 component 2, investment 1.4 – D.D. 1033 17/06/2022, CN00000023).

References

[1] H. Boyes, B. Hallaq, J. Cunningham, and T. Watson, "The industrial internet of things (IIoT): An analysis framework," *Computers in Industry*, vol. 101, pp. 1-12, 2018.

[2] C. U. Bas and S. C. Ergen, "Ultra-wideband Channel Model for Intra vehicular Wireless Sensor Networks Beneath the Chassis: From Statistical Model to Simulations," *IEEE Transactions on Vehicular Technology*, vol. 62, no. 1, pp. 14–25, Jan. 2013.

[3] G. Paolini et al., "RF-Powered Low-Energy Sensor Nodes for Predictive Maintenance in Electromagnetically Harsh Industrial Environments," *Sensors*, vol. 21, no. 2, pp. 386–403, Jan. 2021.

[4] E. Augello, F. Benassi, G. Paolini, D. Masotti and A. Costanzo, "Optimizing Sensors Placement and Wireless Power Transfer in Harsh Electromagnetic Environments," *2024 IEEE International Symposium on Measurements & Networking (M&N)*, pp. 1-6, Rome, Italy, 2024,.

[5] K. Li, W. Ni, L. Duan, M. Abolhasan, and J. Niu, "Wireless Power Transfer and Data Collection in Wireless Sensor Networks," *IEEE Transactions on Vehicular Technology*, vol. 67, no. 3, pp. 2686-2697, Mar. 2018.

[6] M. Luo and K. M. Huang, "Prediction of the electromagnetic field in metallic enclosures using artificial neural networks," *Progress In Electromagnetics Research*, vol. 116, pp. 171-184, 2011.

[7] E. Bleszynski, M. Bleszynski, and T. Jaroszewicz, "A fast integral equation solver for electromagnetic scattering problems," in *IEEE Antennas and Propagation Society International Symposium and URSI National Radio Science Meeting*, Seattle, WA, USA, 1994, vol. 1, pp. 416–419.

[8] E. Augello, F. Benassi, D. Masotti and A. Costanzo, "An Efficient Approach for a Digital Twin model of Harsh EM Environments," *2024 IEEE International Symposium on Antennas and Propagation and INC/USNC-URSI Radio Science Meeting (AP-S/INC-USNC-URSI)*, pp. 1-2,Firenze, Italy, 2024.

[9] Z. Liu, X. Jiang, H. Luo, W. Fang, J. Liu, and D. Wu, "Pool-based unsupervised active learning for regression using iterative representativeness diversity maximization (iRDM)," *Pattern Recognit. Lett.*, vol. 142, pp. 11-19, Feb. 2021.

[10] D. Arthur and S. Vassilvitskii, "K-means++: The Advantages of Careful Seeding," in *SODA '07: Proceedings of the Eighteenth Annual ACM-SIAM Symposium on Discrete Algorithms*, 2007, pp. 1027–1035.

[11] T. Akiba, S. Sano, T. Yanase, T. Ohta, and M. Koyama, "Optuna: A Next-generation Hyperparameter Optimization Framework," in *Proceedings of the 25th ACM SIGKDD International Conference on Knowledge Discovery & Data Mining (KDD '19)*, 2019, pp. 2623–2631

[12] B. Ding, H. Qian, and J. Zhou, "Activation functions and their characteristics in deep neural networks," in 2018 Chinese Control And Decision Conference (CCDC), Shenyang, China, 2018, pp. 1836-1841.